

**Invited Paper****Spectrally-Shaping Viscoelastic Finite-Difference Time Domain Model of a Membrane**Rolf Bader<sup>†</sup>

<sup>†</sup>Institute of Systematic Musicology  
 University of Hamburg  
 Neue Rabenstr. 13, 20354 Hamburg, Germany  
 R.Bader@t-online.de

**Abstract** - The damping of musical instruments is spectrally-shaped, showing beatings and non-exponential decay. Such behaviour can be explained by viscoelastic damping, which also shows spectral sidebands and mode coupling. Previous physical models of musical instruments do only roughly implement viscoelastic damping. The present Finite-Difference Time Domain spectrally-shaping viscoelastic model on the other hand models complex damping spectra as physically reasoned viscoelasticity discussing a membrane. The model assumes a memory, delaying the strains of previous time points, while convolving these strains with a damping function, only to add it to the present stress. It therefore uses a complex Young's modulus and a complex tension, where the real part represents damping. The damping function is calculated as the inverse Laplace transform of the complex Young's modulus spectrum. Contrary to modal analysis, the resulting amplitude decay of a damped target frequency is not exponential. This is in accordance with the physics of viscoelasticity acting with a memory. Amplitude and frequency modulations are found, leading to sidebands in the spectrum. The damping frequency width  $Q$  of neighboring frequencies damped by a target frequency is discussed. A sharper  $Q$  with longer memory and smaller inverse Laplace transform real kernel constant  $\gamma$  is found as expected.

**Keywords:** Physical Modeling, Musical Instrument Acoustics, Viscoelastic Damping, Finite-Difference Time Domain Method, Percussion instrument

**1 INTRODUCTION**

A vibrational system has basically two types of damping, an external damping caused by energy loss due to radiation, and an internal damping caused by energy loss within the structure. The reasons for the internal energy loss are not perfectly clear [17]. There are thermodynamic losses [15] of several kinds, viscoelastic losses due to shearing, atomistic and quantum mechanical considerations of molecular restructuring [9] [21] next to other explanations. Thermal losses expect materials with a higher thermal conductivity to be damped stronger. But although e.g. a metal plate has higher thermal conductivity than a wooden plate, the wooden plate is damped stronger. Therefore thermal losses are expected not to be the major contribution to internal losses. The present paper discusses internal losses due to viscoelasticity only.

Physical models of the drum have been performed for Indian drum heads [19], the snare drum [7], or the bass drum

[3] using Finite-Difference methods. Fractal derivatives have been suggested to replace complex models by single, but fractal derivatives. These lead to a power law of damping [13]. Chaigne uses a Maxwell time-dependent model for damped plates [8] with still considerable differences between model and experiment.

All these models do not allow for a spectrally-shaping viscoelastic damping in the physical model. They only assume an exponential damping curve depending on frequency. Basically two damping terms are used as part of the differential equation, a first-order time derivative of the dependent variable multiplied by a damping constant, and a first-order time and second-order spatial derivative of the dependent variable with plates or membranes. In the first case a perfect exponential damping depending of frequency results. In the second case higher frequencies are damped stronger, compared to the perfect exponential decay case [8]. The second case becomes necessary in cases with strong viscoelasticity.

Nevertheless, the damping behaviour of material used for musical instruments like wood or leather has a complex frequency-dependency. Although exponential in general, some frequency bands might be damped stronger, some weaker, compared to the perfect exponential damping. This is assumed to contribute strongly to the 'liveliness' of wood or leather as material for musical instruments. Guitars built of plastic, like e.g. the Maccaferri plastic guitar, are often perceived to sound plastic, and are therefore rejected [12]. The material property of a spectrally-shaping viscoelastic damping is therefore crucial when replacing traditional material with polymer or hybrid material.

This also holds for physical models of musical instruments, which need to sound as realistic as possible. Using a spectrally-shaping viscoelastic damping method in the models allows for a realistic reproduction of musical instrument sounds. The role of internal damping has not been in the focus of musical acoustics over the last decades. Still as models improve in quality, the differences between real and modeled instruments still existing seem to be caused to a great extent by the lack of a spectrally-shaping viscoelastic damping model.

Experimental data of viscoelastic losses in leather show an increase of damping with higher temperatures above its glass transition temperature [11] which are additionally frequency dependent. Higher water content of leather also leads to higher internal damping. The reasons for such a damping behavior are mainly thought to be a reconfiguration of collagen fibers, within them and between the fibers, where water

molecules become part of the collagen structure [11]. Collagen is a very stiff protein and therefore leather is basically considered a crystal. Still the layering of leather fibers allows gaps which are filled by water, as well as by molecules which are introduced by the process of tanning. Here water molecules enter in two ways, either as larger portions between collagen fibers or as single molecules between or even within collagen molecules. The former is responsible for leather to freeze to a hard plate around zero degree Celsius. The other water molecules lead to a slow melting process around a certain temperature, adding most to the strong viscoelastic properties of leather. Additional components of this viscoelastic internal damping are sudden changes in the molecular geometries when stress is applied. All these processes lead to a phase shift between stress and strain which again leads to an internal energy loss of the vibration. Internal damping can be very strong and therefore contributes considerably to the timbre of a drum built of leather.

Basic models of viscoelastic damping have mainly been discussed with Finite-Element Methods [24]. Here the Maxwell and the Kelvin-Voigt model for relaxation and creep respectively are normally used as time integration models, where combinations of both are able to build arbitrarily complex damping behavior. Both creep and relaxation may have very short but also very long time constants. Guitar builders speak of the 'flowing' of wood when the tension the strings apply to the soundboard leads to a plastic strong deformation of the soundboard over years. Relaxation appears with musical instruments which have plates under tension, like top and back plates of guitars or a crowned piano soundboard. Instrument builders often estimate that the internal tension relaxes over about one year and the deformation due to tension becomes again a plastic deformation with no internal tension left.

Sound absorbing material research uses mainly bitumen-, liquid- and nanotube-based materials [25]. The modeling in this field is nearly exclusively done using the Maxwell or the Kelvin-Voigt model. Again damping is strongest when the operation temperature of the material meets the glass-transition temperature. Complex frequency- and temperature-dependent damping curves appear with sandwich plates [26]. Using a center-finite-difference method [27] shows the appearance of frequency band-gaps in periodically stiffened plates, still here caused by the periodicity of the material and not mainly by viscoelastic effects. The methods used are modal analysis and do not consider the development of the damped amplitudes.

The complex nature of internal damping also appears with wood. In a review paper [5] finds a close correlation between Young's modulus and the damping parameter  $\tan \delta$  for 450 wood species, the relation between imaginary and real parts of a complex Young's modulus, an index often used when measuring viscoelasticity. This index is not taking frequency-dependence of damping into consideration. Damping correlates with Young's modulus, but not with wood density [6]. Comparing normal and compression wood, where the amount of cellulose is higher, it appears the the micro fiber angle (MFA), the angle the cellulose fibers lay inside the second cell wall correlate with both, Young's modulus and damping

[4]. Obataya et al. investigate the influence of viscoelasticity to the vibration of reeds [16].

Viscoelasticity may also vary over musical instrument geometries. Adding additional paste to a drum head is a common practice for drums in Southeast Asia. Indian drums, especially *tablas* are studied in terms of the additional mass added to their drum head [19] [18] called *sihai* which is placed concentric for the *dayan* and off-centric for the *bayan* drum. Varying the width, position, smoothness and strength of the *sihai* it was found that the harmonic overtone relations of the drum modes change and can meet values very close to harmonic ratios.

*Tablas* have a clear pitch, still they are not played as melody instruments. The Myanmar drum circle *pat wain* on the other hand needs to be tuned to pitches over about three octaves [1]. The paste adds considerable viscoelasticity to the drum, next to the leather the drum head is built of. Experimentally it was found that a double-headed drum, like the *pat wain* shows a coupling of the drum heads for lower modes, while the higher modes are more or less decoupled [22] [18]. Normally the upper drum head is keeping its frequency at the lower modes while the lower drum head is forced into the motion and frequency of the upper one.

Several other studies deal with drums. The vibration of the Karen bronze or 'frog' drum has been studied experimentally [14], finding complex modes up to 3 kHz. The influence of non-uniform tension of a drum head was studied using laser-interferometry measurements, where degenerated modes have been found [23] mostly leading to musical beats. The eigenmodes of the drum vessel were analyzed using Finite-Element methods [10]. The coupling between the drum head and the wooden shell was investigated using Finite-Elements for a bass drum [3].

The model presented allows for a very precise computer simulation of vibrational systems in general, using a drum as an example. As internal damping shapes the overall spectral amplitude shape of sounding objects considerably, the suggested model in future can also be used in sound design, sonification, auralization, room acoustics, or in urban environmental noise problems. These topics have become an intense focus of modern engineering over the last years, where simple estimations of overall energy, roughness, sharpness, or brightness of a sound are way not enough to satisfy modern auditory demands. As musical instruments have always been subject to very precise tuning of timbre they are an excellent benchmark.

The method of using Finite-Difference Time Domain (FDTD) sound synthesis belongs to the analysis-by-synthesis approach. It is an alternative to the analyzing branch of information processing, taking existing sounds and deriving their properties using spectral analysis or related techniques. The model approach on the other side gives detailed insight into the material and geometrical properties of the objects, and therefore allows the formulation of a state-space of all possible sounds. Such a state-space can then be used to understand existing sounds with respect to their physical sources, and therefore help to classify and identify sounds with analytical information processing tools much easier. This makes an interplay

between the two analysis ways possible, the forward synthesis and the backward analysis techniques. Such model tools will be subject to machine learning based on physical modeling in the near future. Still this interplay can only reasonably work when using physical models, taking all crucial parameters into consideration. As internal damping strongly shapes the sound of musical instruments, as well as all sounding objects in a frequency-dependent way, without such a model as presented here a precise relation between physics and analysis can only be rough. Due to the complex nature of internal viscoelastic damping such a model is complex too. Additionally, the literature in this field is scarce. The present model is a suggestion to fill this gap to some extent.

First the paper considers viscoelasticity as a frequency-dependent spectrum of a Young's modulus, as known from literature, and later the stiffness of a membrane. Transferring the equations into the time-domain is done via an inverse Laplace transform. Results for a reduced system, a 0-dimensional mass-spring system are discussed, showing complex decay behavior, as well as sidebands with strong damping. Then results for the membrane are shown, estimating the damping strength in correlation with the input parameters of the model as well as the damping frequency width, the impact of a damped target frequency onto its neighboring frequencies.

## 2 METHOD

### 2.1 Viscoelastic Finite-Difference Model

The drum membrane is modeled as a Finite-Difference Time Domain (FDTD) model, used before in models of whole geometries of a guitar, a violin and several other musical instruments [2]. It is implementing the equation of a membrane with tension  $T(x,y)$ , area density  $\nu(x,y) = m(x,y) / B$ , damping constant  $D$ , and displacement  $u$ , like

$$\frac{T(x,y)}{\nu(x,y)} \left( \frac{\partial^2 u}{\partial x^2} + \frac{\partial^2 u}{\partial y^2} \right) = \frac{\partial^2 u}{\partial t^2} + D \frac{\partial u}{\partial t} . \quad (1)$$

The tension is often called  $T$  in the literature, and  $E$  is denoting the Young's modulus. Both are closely related, as  $E$  is measured in Pascal [Pa], or force per area, and  $T$  is measured in Newton [N]. In viscoelastic literature mainly the Young's modulus  $E$  is used, defined as the proportionality constant between stress and strain. As the differential equation of the membrane can also be interpreted as a stress-strain relation, we discuss the viscoelastic model using Young's modulus  $E$  at first, and later use tension  $T$  or Young's modulus  $E$ , to be close to literature conventions.

The area density  $\nu(x,y)$  depends on the mass  $m$  divided by the area  $B$  of the membrane. As is the case with membranes which are nonuniform in thickness, its mass varies along  $x$  and  $y$ . Therefore  $\nu(x,y)$  depends on space. Also the tension  $T(x,y)$  has a spatial distribution. If a drum is tuned by adjusting tuning pegs at its rim, most often it is not possible to adjust the tuning pegs such, that the drum has a perfectly uniform tension distribution over its whole area. Therefore also the tension  $T(x,y)$  depend on  $x$  and  $y$ . The implemented model therefore allows any density and tension distribution. Still as

the focus of this paper is on the viscoelastic damping, density and tension are kept constant, although the model itself easily allows for complex distributions.

This differential equation of the membrane includes a damping term, which leads to an exponential decay of the drum eigenfrequencies, both in time and in frequency. Each partial is therefore exponentially decaying, and the spectrum of the sound will have an exponential decay towards higher frequencies. All this damping depends on a single variable alone. Still experiments nearly never show such a simple behavior. Although damping roughly behaves exponentially, strong deviations appear from such a simple exponential decay, showing amplitude fluctuations, sudden drops, especially right after tone onset or a decay much longer than expected. Indeed literature shows viscoelastic damping to result in a spectral band-gap, and multiple damped bands end up in a complex amplitude spectrum, as discussed in the introduction.

To account for this, internal damping can be expressed as a complex and frequency dependent Young's modulus  $E(s)$  with the complex frequency

$$s = \alpha + i\omega . \quad (2)$$

Then the stress-strain relation in the frequency domain becomes

$$\sigma(s) = E(s) \epsilon(s) , \quad (3)$$

with stress  $\sigma$  and strain  $\epsilon$ . To implement this in a model, the multiplication in the frequency domain can be transformed into the time-domain as a time convolution like

$$\sigma(t) = \int_0^\infty \epsilon(t - \tau) h(\tau) d\tau . \quad (4)$$

Here  $h(\tau)$  is a function representing the time domain of the complex Young's modulus  $E(s)$ . The present stress is the result of all previous strains weighted by  $h(\tau)$ . An inverse Laplace transform is used to transfer  $E(s)$  into  $h(\tau)$  like

$$h(\tau) = \frac{1}{2\pi i} \int_{s=\gamma-i\infty}^{s=\gamma+i\infty} E(s) e^{s\tau} ds . \quad (5)$$

Here  $\gamma$  is a constant for all  $\omega$  and need to be chosen such that the solution converges. The choice of  $\gamma$ , together with  $E(s)$ , determines the damping strength, and therefore is chosen to meet a desired damping. Still for all  $E(s)$ ,  $\gamma$  is a constant.

This solution converges to the non-viscoelastic case when  $E(s)$  does not have any real part. In this trivial case with constant Young's modulus  $E_0$  the inverse Laplace transform is

$$h(\tau) = E_0 \delta(\tau) , \quad (6)$$

where  $\delta(t)$  is the Kroneker delta function with  $\delta(0) = 1$  and  $\delta(\tau \neq 0) = 0$ . An unusual material with internal damping only at frequency  $\omega_0$  has

$$h(\tau) = E_0 \delta(\tau) + \text{Re}\{E(s)\} e^{s\tau} , \quad (7)$$

with damping amplitude  $\text{Re}\{E(s)\}$ .

Therefore a frequency-dependent internal damping spectrum can be written like

$$h(\tau) = \int_s \operatorname{Re}\{E(s)\} e^{s\tau} ds . \quad (8)$$

Each spectral component of a sound is damped with its own damping parameter  $\mu(s)$  and therefore has a time series like

$$u(s, t) = A(s) e^{-\mu t} e^{s \omega t} . \quad (9)$$

Note that it is necessary to clearly distinguish between the real part of the Young's modulus  $\operatorname{Re}\{E(s)\}$ , the real part of the inverse Laplace integrations  $\gamma$ , and the decay  $\mu$ .  $\operatorname{Re}\{E(s)\}$  is a material property, the viscoelasticity of the vibrating material.  $\operatorname{Re}\{E(s)\}$  can be measured experimentally by examining the phase relation between stress and strain of a material under vibration of frequency  $s$ .  $\gamma$  is a signal processing tool which defines the frequency range, or the filter  $Q$  of damping. Indeed real viscoelasticity appearing at a certain frequency has also a  $Q$ -value. Therefore also this parameter can be measured. Still as additional sound properties appear with viscoelasticity, like amplitude modulation, side bands or mode coupling, defining a simple filter  $Q$  is only a rough approximation of the viscoelastic behaviour. Therefore the relation between  $\gamma$  and  $Q$  is not straightforward. Finally,  $\mu$  is only an analysis parameter, the damping exponent of the resulting time series, as best fit to the decay of the respective frequency. Again as the real damped time series shows beatings and non-exponential decay behaviour,  $\mu$  is a rough estimate. Eq. 9 is therefore an oversimplification of the real process, and therefore  $\gamma$  will only be a rough estimation of the general decay of single frequencies. Only the whole viscoelastic equation is suitable to model real behaviour, which is caused by the combination of  $\operatorname{Re}\{E(s)\}$  and  $\gamma$ .

## 2.2 Complex Young's Modulus and Complex Tension

There is a temporal delay between stress and strain which can be expressed as an angle  $\delta$ , the phase relation between stress and strain for a single frequency.  $\delta$  is often measured as this phase relation, and in the literature often written as

$$\tan \delta = E_I/E_R , \quad (10)$$

the relation between the imaginary and real parts of the complex Young's modulus.

The stress-strain relation is also the definition of the Young's modulus. In the case of a membrane we do not have a Young's modulus, so we need to transfer the idea.

Strain is dimensionless and refers to the potential energy of the system caused by displacement differences. The stress is weighted force applied to the structure in order to obtain the strain. In the dynamical case this force can have different parts, the acceleration of the system, damping, or external forces. The unit of the Young's modulus is that of stress, force over area, as strain is dimensionless.

The stress-strain relation is therefore a force balance, according to Newton's idea of mechanical systems in which all interactions can be written as a sum of forces (actio-reactio).

Therefore it is straightforward to replace the strain with the spatial differentiation of the membrane, another force term, and the Young's modulus by force over area density. As the area density is hardly complex, clearly the tension is the parameter we can refer to as complex and frequency dependent. Then the viscoelastic membrane equation reads

$$\int_{\tau=0}^{\infty} h(\tau) \frac{T(x,y)}{\nu} \left( \frac{\partial^2 u(x,y,t-\tau)}{\partial x^2} + \frac{\partial^2 u(x,y,t-\tau)}{\partial y^2} \right) d\tau = \frac{\partial^2 u(x,y,t)}{\partial t^2} . \quad (11)$$

Note that in this equation the damping term with damping constant  $D$  and first derivative of displacement with respect to time was omitted, as it is no longer necessary. All damping can be modeled using the viscoelastic term. Still viscoelasticity is not the only cause for damping. Another major damping is that of radiation loss. This again is complex and beyond the scope of this paper. Due to complex mode shapes, the radiation loss of complex geometries can be calculated analytically only for very simple geometries. There is no general analytical solution. Still roughly this damping is exponential with respect to frequency. Therefore one might still keep the first-order differential term with respect to time as a damping term of external damping.

## 2.3 Analytical Proof of Non-Exponential Time Decay of Viscoelastic Damping

Now we can analytically decide, if the viscoelastic decay is exponential in time or not. Solving this equation is not trivial, both for the spatial part  $v(x,y)$  as well as for the temporal  $w(t)$  with

$$u(x,y,t) = v(x,y) w(t) . \quad (12)$$

As we are interested in the temporal development of single frequencies, we can leave the exact solution of  $v(x,y)$  for a later stage, and assume that when finding this solution, which is subject to some boundary condition, it can be differentiated with

$$\frac{\partial^2 w(x,y)}{\partial x^2} + \frac{\partial^2 w(x,y)}{\partial y^2} = b(s) w(x,y) , \quad (13)$$

where  $b(s)$  is a constant depending on  $s$ . Then Eq. 11 simplifies to

$$\frac{T(x,y) b(s)}{\mu} \int_{\tau=0}^{\infty} h(\tau) w(t-\tau) d\tau = \frac{\partial^2 w(t)}{\partial t^2} . \quad (14)$$

Basically,  $b(s) w(x,y)$  could be the solution of any set of linear differential equations, and we will use this later, studying the model with a 0-dimensional mass-spring system. The viscoelastic model for such a system would be

$$K \int_{\tau=0}^{\infty} h(\tau) w(t-\tau) d\tau = \frac{\partial^2 w(t)}{\partial t^2} , \quad (15)$$

where  $K$  is the spring stiffness.

It is interesting to see that inserting the expected exponential damping solution into Eq. 14 or Eq. 15, similar to Eq. 9,

$$w(t) = A e^{-\alpha t} e^{i\omega t} \quad (16)$$

is obviously not solving it. This means that the model of a frequency-dependent viscoelasticity, as time delay of previous strains entering the present stress, does not necessarily lead to the straight solution of an exponential decaying wave.

## 2.4 Memory Effect of Viscoelasticity

This is reasonable when remembering the physical reasoning of viscoelasticity as a delay of previous strains acting to a present stress. Such a system has a memory, and previous vibrations will act on the present one. In most cases this leads to a damping, as the additional acceleration produced by the previous strains counteracts the present acceleration, therefore reducing it and therefore damping the system.

Still the previous strains might also act as an additional acceleration, which then is driving the system. Considering a strong viscoelastic damping, where most of the energy is gone after 10 ms. If the  $h(\tau)$  is longer than 10 ms and still acts until 15 ms, the acceleration supplied by  $h(\tau)$  after 10 ms does not find a vibration on the geometry which it could counteract anymore and will drive the system again. This means that the strain stored in system has a kind of a memory and will act as an energy supply.

This additional energy will again be subject to viscoelastic damping later on again, and so the system will decay on the long run. But in such a situation we would expect an amplitude beating on top of a generally exponential decay. Such amplitude beatings are indeed found experimentally quite often. Of course they may have many reasons, like degenerated or close modes interacting and beating, or like complex couplings in complex geometries which musical instruments most often are. Still viscoelastic damping can also be a source of such amplitude beatings.

To go one step further in this discussion, when increasing the memory time, which in our model is decreasing  $\gamma$ , the amount of stored strain acts will increase the damping but will also increase the driving. Then the total damping behavior will be a combination of damping and driving, and we will expect a peak for strongest damping at a certain value of  $\gamma$ , which we will indeed find in the model results later on. Therefore the relation between the strength of viscoelasticity  $\gamma$  and the resulting decay exponent  $\mu$  is highly nonlinear. Again there is no analytical solution to this relation and therefore one task below is to calculate the relation for a parameter space of both parameters, together with the third parameter changing  $\mu$ , which is the viscoelasticity  $\text{Re}\{E(s)\}$ .

To push this even further, with extreme values of  $\gamma$  we will even expect the driving to be larger than the damping, and the system will not decay but increase in energy. This is no physical case anymore in terms of normal viscoelastic damped systems. Still it is a feature which we might use to model energy supply to a system. Of course this need to be done carefully, as a real energy supply by a string or another coupled part of a musical instrument might follow different rules.

Still the beating found is perfectly physical and known from strongly viscoelastic damped systems, e.g. when rotating an egg. When suddenly rotating an egg with a hand, the hard wall of the egg will follow the acceleration without delay, still the proteins inside the egg are driven only by the eggs

wall and follow the movement only with a visible delay. This takes energy from the wall rotation, and it will slow down considerably. But then one can visually experience the wall to again accelerate, as the energy in the proteins are again acting on the walls with a considerable delay. Then the walls indeed have been accelerated again after some time. Therefore in principle such energy supply due to memory is a physically expected behavior, and might play a role with musical instruments with higher frequencies as we will see in the results section.

## 2.5 Discretization

When implementing the equations on a GPU, the integral cannot be performed over an infinite time span. It is memory expensive to store previous strains for all nodal points of the membrane geometry and perform convolutions for all node points at each calculated time point. Therefore the equation restricts the integration time to T. Additionally the calculation is time discrete. This transforms Eq. 3 into

$$\sigma_t = \sum_{\tau=0}^{N-1} \epsilon_{t-\tau} h_\tau, \quad (17)$$

with strain  $\sigma_t$  at discrete time point t and N samples to use. Also the integral of the discrete viscoelastic function  $h_\tau$  becomes a sum, where only integer multiples of the periodicity  $T = N / r$  at sampling rate r can be used like

$$h_\tau = \frac{1}{2\pi i} \sum_{k=1}^N E_k e^{\gamma \tau/r} e^{i \omega_k \tau/r}, \text{ with } \tau = 0, 1, 2, 3, \dots, N-1 \quad (18)$$

where  $E_k$  are now the discrete complex values for frequencies

$$\omega_k = 2\pi k / r \text{ with } k = 1, 2, 3, \dots, N. \quad (19)$$

As the calculation itself is kept in the time domain,  $h(\tau)$  need to be real and therefore is rewritten like

$$h_\tau = E_0 \delta(\tau) + \frac{1}{2\pi} \sum_{k=1}^N \text{Re}\{E_k\} e^{\gamma \tau/r} \sin(\omega_k \tau/r + \phi_k), \quad (20)$$

with  $\tau = 0, 1, 2, 3, \dots, N-1$

The Kroneker delta function sums up all imaginary parts of the  $E_k$  and for itself behaves like the non-viscoelastic case, as shown above. The following sum can be performed only for those  $\omega_k$  where  $\text{Re}\{E_k\} \neq 0$  and is zero for all others. The sine functions need to be used for the transient case, where a drum is hit by a stick, or a guitar string by a finger, etc. There, starting from  $t = 0$ , the strains only build up, starting from  $\epsilon(0) = 0$ . Then the phase  $\phi_k = 0$ . When using a cosine term, the convolution would be out of phase with the strains and therefore no viscoelastic damping can occur. Depending on the musical instrument investigated,  $\phi_k$  can be any function, in the present study  $\phi_k = 0$  for all k.

Note that the Young's modulus in the case of no viscoelastic damping is now purely imaginary instead of real and only

get a real part when viscoelastic damping takes place. The reason is the use of  $s = \alpha + i\omega$ , where  $\omega$  is the frequency and  $\alpha$  the damping. This is no loss of generality, as also stress and strain are defined as functions of  $s$  like  $\sigma(s)$  and  $\omega(s)$ , and therefore in terms of no viscoelastic damping their relative phases are zero as physically true.

Now as total damping consists of internal plus radiation damping, a term for modeling radiation damping is missing. The omitted temporal derivative term would not serve here well, as radiation damping is only roughly related to a simple exponential decay, the derivative term leads to, as discussed above. Radiation loss depends on the eigenmode shape of the radiating body and therefore also need to be modeled frequency-dependent, just like internal damping. Radiation damping could therefore be modeled geometrically by adding the air volume around the drum to the model. Still this would make computational time very much higher.

Still radiation loss can be calculated in alternative ways. If the geometry is simple, like with a circular drum, radiation loss can be calculated analytically. Alternatively, radiation loss can be calculated for more complex geometries when the vibration modes are known. Then radiation can be calculated as forward propagation by integrating the mode vibration into the air surrounding the drum. The amount of cancellation of energy due to phase differences in the modes determines the energy loss of this mode due to sound radiation. As the Finite-Difference model suggested here calculates the mode shapes anyway, this approach can be used to determine the energy loss due to radiation.

In this paper we are interested in viscoelastic damping alone. Addition other dampings would make the solution a combination of them and it would be hard to distinguish the strength of each damping one from another.

## 2.6 Membrane Model Properties

A circular drum was modelled with a radius of 10 cm a membrane tension  $T = 1.7 \times 10^6$  N and an area density of  $\mu = 10^{-3}$  kg / m<sup>2</sup> which results in a fundamental frequency  $f_0 = 306$  Hz for the undamped membrane. A regular rectangular grid of  $104 \times 104$  nodal points was used laying over the circular membrane, where only grid points in the membrane area were used. The boundary conditions were fixed, so the displacement at the rim was  $u_{\text{rim}} = 0$ , but all possible slopes  $\frac{\partial u_{\text{rim}}}{\partial x}$  and  $\frac{\partial u_{\text{rim}}}{\partial y}$  were allowed.

Three frequencies were tested, the fundamental frequency  $f_0 = 306$  Hz,  $f_0 = 1092$  Hz and a high frequency  $f_1 = 4174$  Hz. These frequencies are peaks in the undamped membrane and the influence of viscoelastic damping on them was tested.

The calculations were performed on a Graphics Processing Unit (GPU) with massive parallel computation. Still the model is not real-time and - depending on the GPU used - calculating one second of sound with a sample rate of 96 kHz takes between five to ten seconds.

The spatial grid was implemented on the GPU using three vectors of length  $104 \times 104 = 10816$  vector entries, one for displacement, one for velocity, and one for displacement storage. The acceleration memory was implemented as a vector of  $104 \times 104 \times 1000 = 10816000$  entries. The CUDA

language was used, implementing the model on an NVIDIA GTX 1070 GPU on a laptop. The calculations for acceleration at a present time point, for velocity at a present time point, and for viscoelastic damping using the acceleration memory vector were implemented for all 10816 nodal points in parallel. The new accelerations on the grid were added to the end of the circular acceleration memory vector, and the pointer of this vector was shifted by one vector entry. After performing one time step the new calculated displacements were transferred to the displacement storage vector. From this displacement storage vector, in the next time step, the new accelerations etc. were calculated.

## 2.7 Post-Processing

To calculate the exponential decay parameter  $\mu$  from the resulting time series of the model, a Wavelet transform at  $f_0$  was performed using a complex Morlet wavelet. For adjacent time points the amplitude of the peak frequency was taken, resulting in a time series of this peak. An exponential decay of this amplitude leads to a steady slope when taking the logarithm of the amplitude time series, a method well known from room acoustics. This slope was calculated using a linear fit model with the data. With very fast decays only the part of the series was used which lies before the amplitude starts fluctuating strongly (see example below).

As viscoelastic damping applied to a single frequency is partly like a filter, for now simplifying by neglecting the amplitude modulation or the sideband effect, the frequency width of this filter is calculated from the time series too. As we deal with a musical signal having discrete eigenvalues this is not a straightforward process, like it would be when we would consider a continuous spectrum. The only way to estimate the influence of damping of a target frequency  $f_0$  onto a neighbouring frequency  $f_1$  is to calculate both damping coefficients  $\mu_0$  and  $\mu_1$ . In analogy to the filter quality definition of  $Q = f / \Delta f$ , with  $\Delta f$  the frequency width of half the amplitude as the center frequency of the band gap, we define the filter quality  $Q$  like

$$Q = \frac{\mu_0}{\mu_1} / \Delta f, \quad (21)$$

where  $\Delta f = |f_0 - f_1|$ .  $Q$  therefore gets higher with a narrower band gap, as one might be used to from filter  $Q$  values. In cases the neighbouring frequency  $f_1$  is not affected by the damping,  $\mu_1 = 0$ . In these cases calculating  $Q$  from it does not make sense anymore, as this frequency no longer tells about the width of the band gap. In these cases no  $Q$  is displayed anymore. We will have this case below, and as there  $f_1$  is the closest peak next to  $f_0$  we cannot tell about the bandwidth anymore. Still this is not a problem, as defining a band gap only makes sense if there is an effect on neighboring frequencies, which no longer is the case there. These values are therefore of particular interest, in these cases one frequency can be damped without any effect to the rest of the spectrum.

### 3 RESULTS

To test the decay behavior, at first the model is applied to a 0-dimensional mass-spring system. Then results for the membrane are presented, discussing frequency dependency, Q-values, as well as stability.

#### 3.1 Viscoelastic Damping of a Mass-Spring System

The most simple case of viscoelastic damping is that of a mass-spring system of Eq. 15, which is modeled here with  $D= 10^9$  and mass  $m=1$ . The initial values are for the velocity  $v(0) = 0$  and the displacement  $u(0) = 1$ , which were chosen to easily fit an exponential decay curve to the resulting time series  $u$ , starting at  $u(0) = 1$ .

The calculation was performed for four values of  $\gamma = 1, 1/10, 1/40$  and  $1/140$ , as shown in Fig. 1. The respective functions  $h$  are plotted within each case at the right lower corner. To each plot an exponential function was fitted by hand, starting at  $u(0) = 1$  and meeting the next peak. The gray curve is the integral of the viscoelastic force acting back on the respective time point. In the general model  $\sigma = E \epsilon$  the displacement  $u$  would be the stress  $\sigma$ , and the stored acceleration corresponds to strain  $\epsilon$ , which acts on the stress with a memory, the integral of the strains at the previous time points with  $h(\tau)$ . A sample rate of 96 kHz was used in the simulation to be the same as with the following example of a membrane.

Theory expects with no damping ( $\gamma = 1$ ) a phase alignment between stress and strain, which is the case, and can be seen in the top plot of Fig. 1. The small time gap between the two curves comes from the time integration algorithm, delaying the acting integrated strain to the next sample point of the stress.

Also according to theory, with viscoelastic damping, strain and stress are out of phase with the strain leading, as shown with  $\gamma = 1/10$  in the second plot from top. The function  $h(\tau)$  is very short in this case and acts on the strain less than 1 ms. Still the damping is already strong with a fast decay over 5 ms.

Still when fitting an exponential curve to  $u(t)$ , as e.g. with  $\gamma = 1/10$ , the curve does not fit the model results perfectly. The exponent  $\mu$  of this fit was chosen by hand, starting at unity with  $t=0$  and meeting the first peak of  $u(t)$ . With following peaks the error increases. This becomes worse with higher damping case of  $\gamma = 1/40$  (third plot from top).

This deviation of the decay of  $u(t)$  from an exponential decay is even worse for  $\gamma = 1/140$ . Here an amplitude and frequency modulation appears and  $u(t)$  is far from having a simple decay behavior. The deviations of decay in the first two examples  $\gamma = 1/10$  and  $\gamma = 1/40$  are therefore no artifacts of the calculation, but a basic behavior of viscoelastic damping.

The reason for this behavior appears when examining the integrated strain curve in gray e.g. with  $\gamma = 1/140$ . It only increases over two periods, as integration time is relatively long here, and previous  $u(t)$  enter over up to 6 ms. Still damping acts on  $u(t)$  right from the start, decaying  $u(t)$  fast.

Now the damping appears as the stored acceleration over time and is counteracting the acceleration at the present mo-

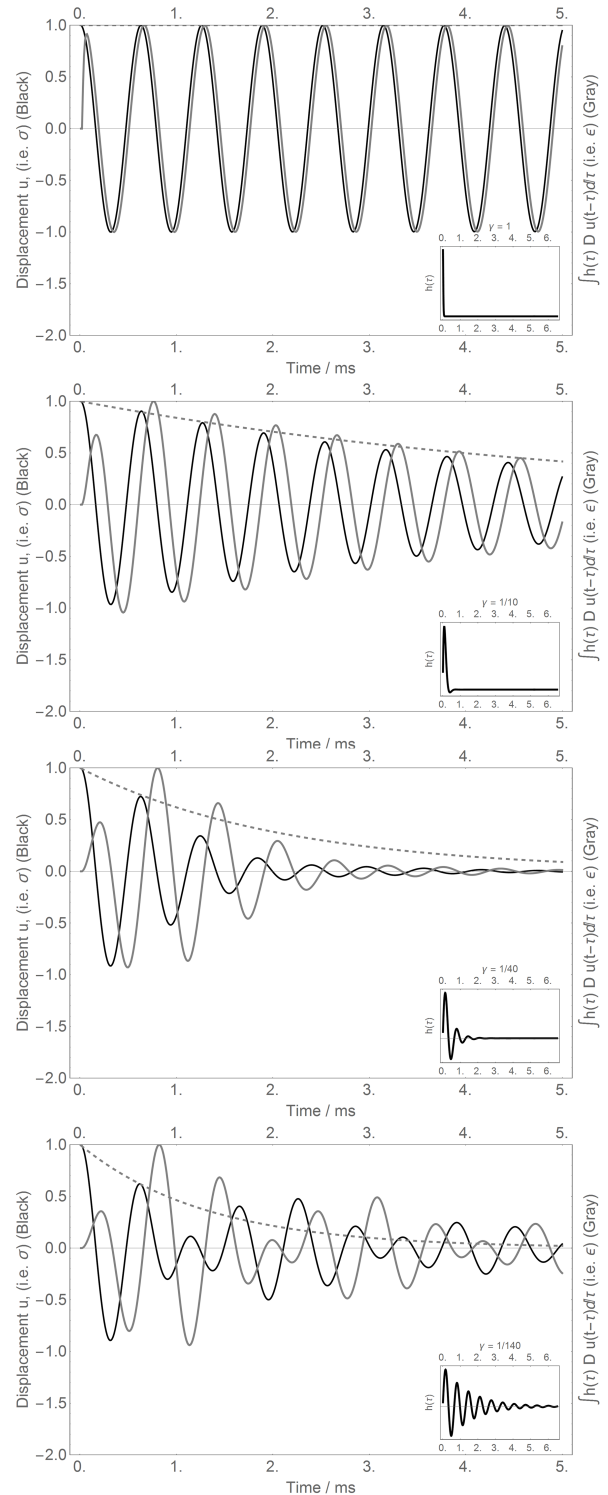


Figure 1: For viscoelastic damped time series  $u(t)$  of a mass-spring system with spring constant  $D = 10^9$  vibrating at 1536 Hz, viscoelastic function  $h$  with a length of 10 periods of  $f$ , and for four inverse Laplace transform real kernel values  $\gamma = 1, 1/10, 1/40$  and  $1/140$  (top to bottom). In each case  $h$  is inserted as a side plot within each case. An exponential fit is applied in all cases by hand to meet the first peak of  $u(t)$ . In all cases such an exponential fit does not meet the results. For smaller  $\gamma$  an amplitude and frequency modulation appears.

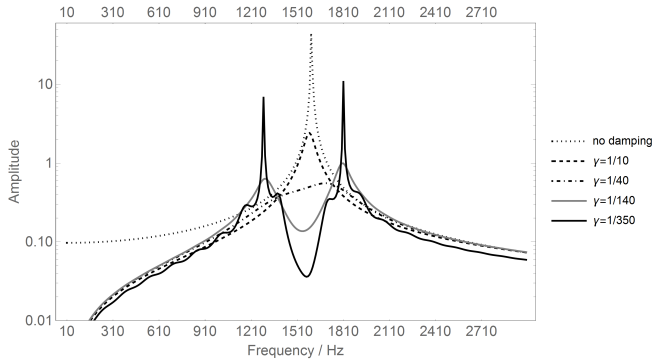


Figure 2: Spectra of the viscoelastic damped mass-spring system shown in Fig. 1 for no damping,  $\gamma = 1/10$ ,  $1/40$ ,  $1/140$  and the additional case of  $1/350$ . The original frequency at  $f = 1536$  Hz is decaying with lower  $\gamma$ . At the same time sidebands appear, which become considerably strong with  $\gamma = 1/350$ . These sidebands are the result of the amplitude and frequency modulation of the decaying time series  $u(t)$  for small  $\gamma$ .

ment damping the system. Still if the system is already damped quite strongly and the stored acceleration is strong too, the counteraction overshoots, and part of the stored acceleration is now no longer acting as damping but as an energy supply. This is a fundamental physical behavior of viscoelastic damping, which was tried to illustrate with the example of the rotating egg above.

The back and forth of damping and enhancing of  $u(t)$  by the integrate d strain in the system leads to an amplitude, but also to a frequency modulation.

Fig. 2 shows the spectra of the time series of Fig. 1 for  $\gamma = 1/10$ ,  $1/40$ ,  $1/140$  and additionally  $\gamma = 1/350$ . The case of  $\gamma = 1$  is plotted too.

The decay at  $f$  clearly becomes stronger with decreasing  $\gamma$ , and the peak is gone with  $\gamma = 1/40$ . Still with  $\gamma = 1/140$  two sidebands appear above and below  $f$ . With  $\gamma = 1/350$  a series of these sidebands appear above and below  $f$ . These are the results of the amplitude and frequency modulation of the mass-spring system by the viscoelastic damping.

Therefore, as a first result of the method we find that a viscoelastic damped system does not have a simple exponential decay, as expected analytically, as shown above. This implies that Eq. 9 is not a solution of the system, which is expected, as it is no solution of the viscoelastic differential equation 11. We therefore find that the naive replacement of a real Young's modulus by a complex one, often assumed in modal analysis, leading to a simple exponential decay of the respective partial may be a good approximation with very slowly decaying modes, but is not sufficient for fast decays. Still most structures of musical instruments, like wooden plates or membranes, especially at high frequencies often have a very fast decay, and therefore can show a very complicated decay behavior and a decay time not meeting that of an exponential decay.

The example is only 0-dimensional. Therefore the appearing side bands clearly come from the modulation of the vibrating point mass. Still with higher-dimensional geometries,

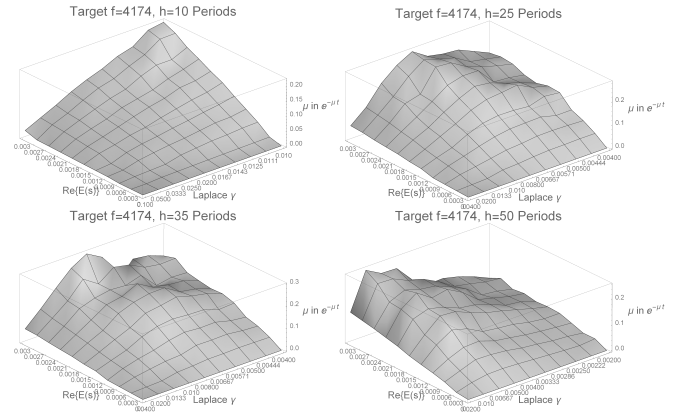


Figure 3: Damping exponent  $\mu$  calculated as interpolation from the time series of the model at  $f = 4174$  Hz for four different amounts of periods of  $f$ : 10, 25, 35 and 50 periods. In each case  $\text{Re}\{E(s)\}$  was increased from 0 to 0.0003 in ten equal steps, and the inverse Laplace real part of integration  $\gamma$  was used from  $1/10$  to  $1/100$  (10 periods),  $1/25$  to  $1/250$  (25 and 35 periods) and  $1/50$  to  $1/500$  (50 periods). These values were used to stay within a stable region of the model. The resulting  $\mu$  have a peak around  $\gamma = 1/150$ , independent from the amount of periods used.  $\mu$  decreases after this peak, indicating a growing influence of driving energy caused by longer delays.

like with the membrane discussed next, the energy of the side bands might meet other vibrating frequencies present at the side band frequencies. Then we have an energy transfer between two modes, a mode coupling. Such a mode coupling is hard to distinguish from other effects in a higher-dimensional geometry. Still as the 0-dimensional case is clearly showing a mode coupling, we do expect such an energy transfer between modes also for all higher-dimensional cases.

### 3.2 Viscoelastic Membrane

To test the membrane model it is damped at one single frequency only, here at  $f_1 = 4174$  Hz, later also at  $f_0 = 1092$  Hz and  $f_0 = 306$  Hz. The model has three tunable parameters for one frequency, the real part of the Young's modulus  $\text{Re}\{E(s)\}$ , the inverse Laplace transform integration real constant  $\gamma$ , and the length of  $h(\tau)$ , the time series corresponding to  $E(s)$ .

As shown with the mass-spring model, the damping is not an exponential decay. Still to arrive at an estimate about the damping strength, such an exponent  $\mu$  is still calculated, using a complex Morlet wavelet transform with a very long wavelet number of 60 wave periods, as discussed above. Other methods could be used, like detecting the last amplitude of the damped frequency in time above a certain threshold. Still with amplitude modulated sounds, easily present in musical instruments, this might lead to artifacts as well. The problem of defining such a parameter is also one of measuring damping from a recorded sound, which is not at all trivial, and beyond the scope of this paper.

Fig. 3 shows all three parameters discussed above changed within a parameter space. Four cases of the length of  $h(\tau)$

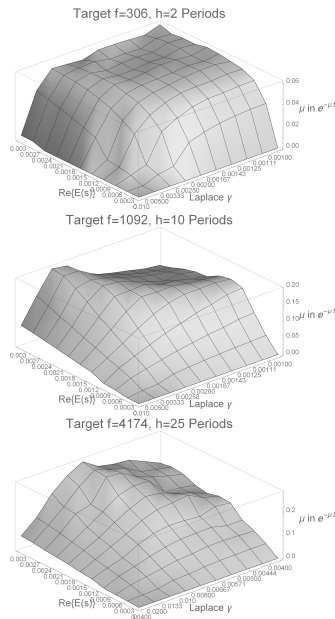


Figure 4: Damping exponent  $\mu$  for three target frequencies damped by the model: 306 Hz, 1092 Hz, 4174 Hz over their stable parameter range for  $\gamma$  and  $\text{Re}\{E(s)\}$ . The basic property of a maximum damping at a certain  $\gamma$  is present in all cases.

are shown in the amount of periods of  $f_1$ , 10, 25, 35 and 50 periods. The up axis is the resulting damping exponent  $\mu$  as calculated from the resulting time series by exponential fit of the amplitudes from the wavelet transform. The other axis are  $\text{Re}\{E(s)\}$ , which in all cases has been varied in ten equal steps from 0 to 0.0003, and the Laplace transform real parameter  $\gamma$ . This has different variations, depending on the amount of periods used, it was varied from 1/10 to 1/100 (10 periods), 1/25 to 1/250 (25 and 35 periods) and 1/50 to 1/500 (50 periods). The parameters were set this way to ensure a stable algorithm. When increasing the parameters beyond the shown region, the resulting time series will constantly and exponentially increase in amplitude, which is unphysical as there is no additional energy supply to the system. In other words, for values beyond the shown parameter spaces the algorithm blows up. Therefore we have a trade-off between stability and computational cost, as longer  $h(\tau)$  means more computation time and memory.

In three cases, 25, 35 and 50 periods, there is a peak of maximum damping  $\mu$ . Damping increases with increasing  $\text{Re}\{E(s)\}$  as expected, but also when lowering  $\gamma$  from high values to lower ones. The peak in all three cases is around  $\gamma = 1/150$ . The 10 period case does not reach this  $\gamma$  and therefore the peak is not present there.

After  $\gamma = 1/150$  the damping exponent  $\mu$  decreases again. This is expected remembering the results of the mass-spring system, as with smaller  $\gamma$  the viscoelasticity also acts as a delayed energy supply. The fact that the peaks of maximum decay  $\mu$  are independent of the length of  $h(\tau)$  is according to theory.

As a consequence one might find that 10 periods are enough for such a frequency, as here the maximum possible damping

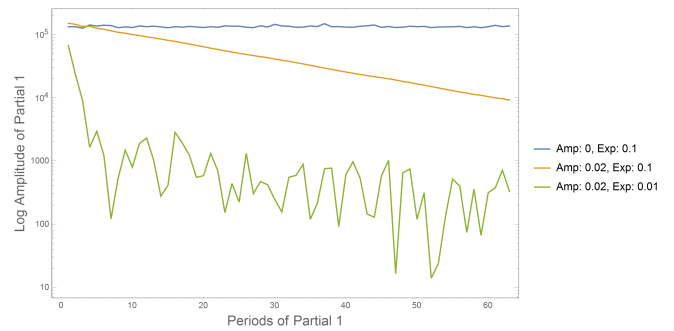


Figure 5: Three examples of the decay of frequency  $f_0 = 306$  Hz for three different cases, a)  $\text{Re}\{E(x)\} = 0$ ,  $\gamma = 1/10$ , b)  $\text{Re}\{E(x)\} = 0.02$ ,  $\gamma = 1/10$ , c)  $\text{Re}\{E(x)\} = 0.02$ ,  $\gamma = 1/100$ . The decays are steady transformed into a decay parameter  $\mu$  by a linear model fit. The case c) has a fast decay and continuous fluctuations afterwards. Here only the beginning has been used to fit the linear decay model.

can be reached, next to all other damping strengths. Still this is not perfectly the case because of two reasons. First, when discussing the filter depth, or filter quality  $Q$  of the model, the length  $h(\tau)$  does play a crucial role, as we will see below. Secondly, the damping curve changes with smaller  $\gamma$  making larger  $h(\tau)$  necessary. Therefore when reproducing a complex damping amplitude decay curve, this might only be possible using small  $\gamma$  for which large  $h(\tau)$  are needed.

A maximum  $\mu$  at a certain  $\gamma$  found with 4174 Hz is also true for other frequencies. In Fig. 4 three cases are shown, for 306 Hz ( $\gamma$  from 0.001 to 0.01), 1092 Hz ( $\gamma$  from 0.004 to 0.04) and again for 4174 Hz ( $\gamma$  from 0.004 to 0.04) with  $\text{Re}\{E(s)\}$  from 0 to 0.0003 in ten steps in all cases. The maximum damping  $\mu$  in the resulting time series at a certain  $\gamma$  is present in all cases. This feature holds over the whole frequency range as expected, although  $\gamma$  becomes larger with lower frequencies.

The decay of three examples for the case of  $f_0 = 306$  Hz are shown in Fig. 5. The plot displays the peak amplitudes over time for adjacent periods of  $f_0$ . The amplitude axis is logarithmic, therefore with an exponential decay a straight line with a constant slope is expected. In the first case of no damping the slope is zero. For the second case of a slightly damped  $f_0$  the slope is very constant and the decay does not deviate from a simple exponential one considerably. Titting a  $\mu$  to this decay is therefore straightforward. Still the third example shows a very fast decay, followed by an amplitude fluctuation which is overall decaying but much slower than its beginning. The fluctuations are no noise, as the amplitude is not small enough to end in discretization noise. Also the periodicity is quite regular and starts at the fast decay part already. This is an example of a complex damping and closely aligns with the results from the mass-spring model.

### 3.3 Damping Frequency Width $Q$

When damping a spectrum at a certain frequency, neighboring frequencies will be effected too. This corresponds to filter theory, where the width of the filter might be defined as  $Q = \Delta f / f$ , where  $f$  is the frequency and  $\Delta f$  is the frequency

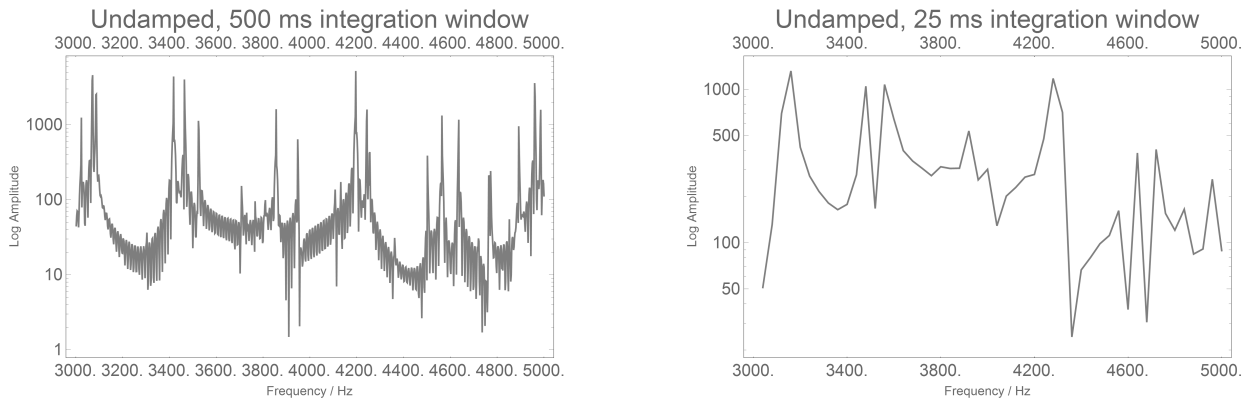


Figure 6: Spectra of the frequency region around  $f = 4174$  Hz over an FFT length of 500 ms (left) and 50 ms (right). The peaks resolved for 500 ms are blurred for 50 ms. As the length of  $h(\tau)$  is between 1 and 6 ms, the damping algorithm deals with the blurred case. Therefore the neighbouring frequencies  $f_1 = 3860$  Hz and  $f_2 = 4587$  Hz were used for calculating the damping frequency width  $Q$ .

width over half the amplitude of neighboring damping. As discussed in the methods section, this definition cannot trivially be transferred to the present case, as we do not have a continuous spectrum, but one consisting of discrete mode frequencies. Therefore the damping of the neighboring frequencies  $f_1$  and  $f_2$  below and above the damping target frequency  $f$  are taken as a reference for the damping frequency width  $Q$ .

In the present case, again looking at 4174 Hz as the target frequency, a bundle of single frequencies are present. Still only when using a large Fourier transform window of about 500 ms these single frequencies are resolved. As the length of the function  $h(\tau)$  has a maximum of about 6 ms and often is less than 1 ms, these single frequencies are not resolved during the damping process. Therefore in the analysis the broader peak around  $f = 4174$  Hz,  $f_1 = 3860$  Hz and  $f_2 = 4587$  Hz are taken. The frequencies were calculated using again the Wavelet transform using a wavelet number of 5, and detecting the frequencies at amplitude maxima of the blurred spectral peaks.

In Fig. 7 and Fig. 8 the  $Q$  for the case of  $f = 4174$  Hz and the two neighbouring frequencies  $f_1$  and  $f_2$  are shown. Both compare  $f$  once with  $f_1$  (left plot each) and  $f$  with  $f_2$  (right plot each). Each line represents changing  $\text{Re}\{E(s)\}$  for one  $\gamma$ .

Overall with decreasing  $\gamma$ ,  $Q$  increases. This means that when the function  $h(\tau)$  decays slower, the sharpness of damping improves. This is expected and is analog to filter theory. The dependency of  $Q$  on  $\text{Re}\{E(s)\}$  may be neglected, like with the 10 period case for  $f_1$  (first figure, left plot). Still in the case of  $f_2$  there clearly is a dependency on the real part of the complex Young's modulus, still not a trivial one.

The reason for this behavior could be found in the fact that the target frequency damping effects all peaks present in the peak bundle around  $f_2$ , which results in a complex amplitude modulation of  $f_2$ , caused by the beating of frequencies. As these single frequencies in the bundle are damping with a different amount, depending on their distance from  $f$ , the amplitude modulation is not constant and might become very complex. Then fitting a simple exponential decay to such a

complex decay could lead to such a behavior.

When examining the 50 period cases, although the basic pattern of increased  $Q$  with decreased  $\gamma$  continues, the plot looks more complex than for the 10 period case. The reason is that with longer  $h(\tau)$  the amplitude beating, as discussed with the mass-spring system, is getting more and more prominent. Combined with the very fast decay of the partial and the problem discussed above with the beating within the frequency bundle, the fit of the decay to a simple exponential fit will again cause such a complex pattern.

In the 50 period plots we also find some curves not complete and ending at some  $\text{Re}\{E(s)\}$  with no values on the left anymore. This are the cases where there is no damping of  $f_1$  or  $f_2$  anymore when damping  $f$ , and therefore  $Q$  becomes infinity (not displayed). These cases are particularly interesting, as they mean a very sharp  $Q$  with no influence of the target frequency on neighbouring frequencies.

Similar results appear for the 25 period and 35 period case at this frequency, therefore displaying the results is omitted here. A gradual transition from 10 period with fairly ordered curves to 50 period with more complex behavior can be observed with the 25 and 35 period cases.

## 4 CONCLUSION

When implementing viscoelastic damping as a memory effect in the time-domain, the resulting amplitude drop of the damped frequencies is not a simple exponential decay. With small viscoelastic effects and long decay times the difference between the real and the exponential decay might be small. Still with strong damping present in wood or leather, an exponential decay rate is no longer a good approximation.

Furthermore, due to the memory effect beatings appear in the decay due to energy supply from the memory to the present vibration, leading to an amplitude increase. This leads to an amplitude and frequency oscillation and therefore to sidebands in the spectrum. These sidebands mean an energy transfer from the target frequency of damping to neighboring frequencies which causes a mode coupling.

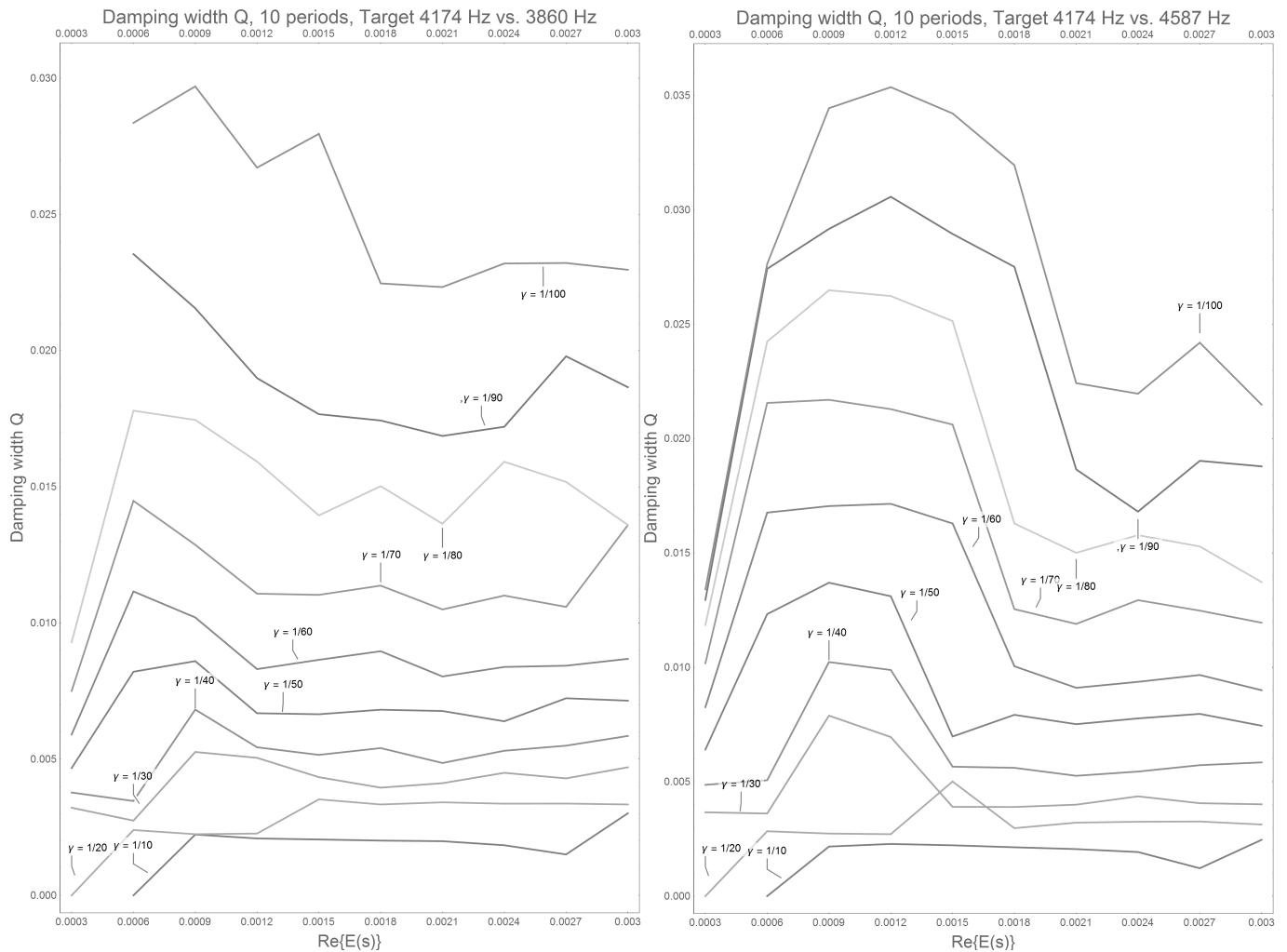


Figure 7: Damping width  $Q$  for the 10 period case comparing the target frequency  $f$  with  $f_1$  (left plot) and  $f_2$  (right plot). In both cases  $Q$  increases with decreasing  $\gamma$ , therefore lowering the damping of the neighboring frequencies when damping the target. For  $f_2$  a dependency of  $Q$  on  $\text{Re}\{E(s)\}$  appears which is not so prominent with  $f_1$ .

Also the length of the memory in most viscoelastic cases is very short, it might be below 1 ms, maybe up to 6 ms (although the time constant of viscoelastic damping might be up to weeks or years as discussed in the introduction). But within very short time scales the frequency range of damping has a certain width, and therefore a damping width  $Q$  can be defined as the relation of damping strength of the target frequency to neighboring frequencies. This damping width is larger with smaller damping functions  $h(\tau)$  and smaller exponents  $\gamma$  as expected. Still this damping width also means that many peaks in this regions are damped simultaneously, but with different strength, depending on their distance to the target frequency. This leads to very complex amplitude beatings in these regions during the decay.

Many of these damping behavior found, like a very sharp decay right after the beginning of the sound followed by a slower decay with amplitude beating, are present in real musical instrument recordings. Such sounds are found with percussion instruments like the xylophone, bass and snare drums of a modern drum kit, or with wood blocks. They are also found with harps, flamenco guitars, or upright pianos. All

such instruments have a complex initial transient, followed by a pitched decaying sound. Still there are many other reasons for amplitude decay, like radiation damping, energy conversion between modes, or related things. Still viscoelastic damping is one of the components leading to such behavior.

After understanding the behavior of viscoelastic damping in terms of the amplitude decay, the next step is to model the recorded damping of a real guitar top plate or piano soundboard with the viscoelastic damping model. This is work for future projects.

## ACKNOWLEDGEMENTS

The work was funded by Deutsche Forschungsgemeinschaft (DFG).

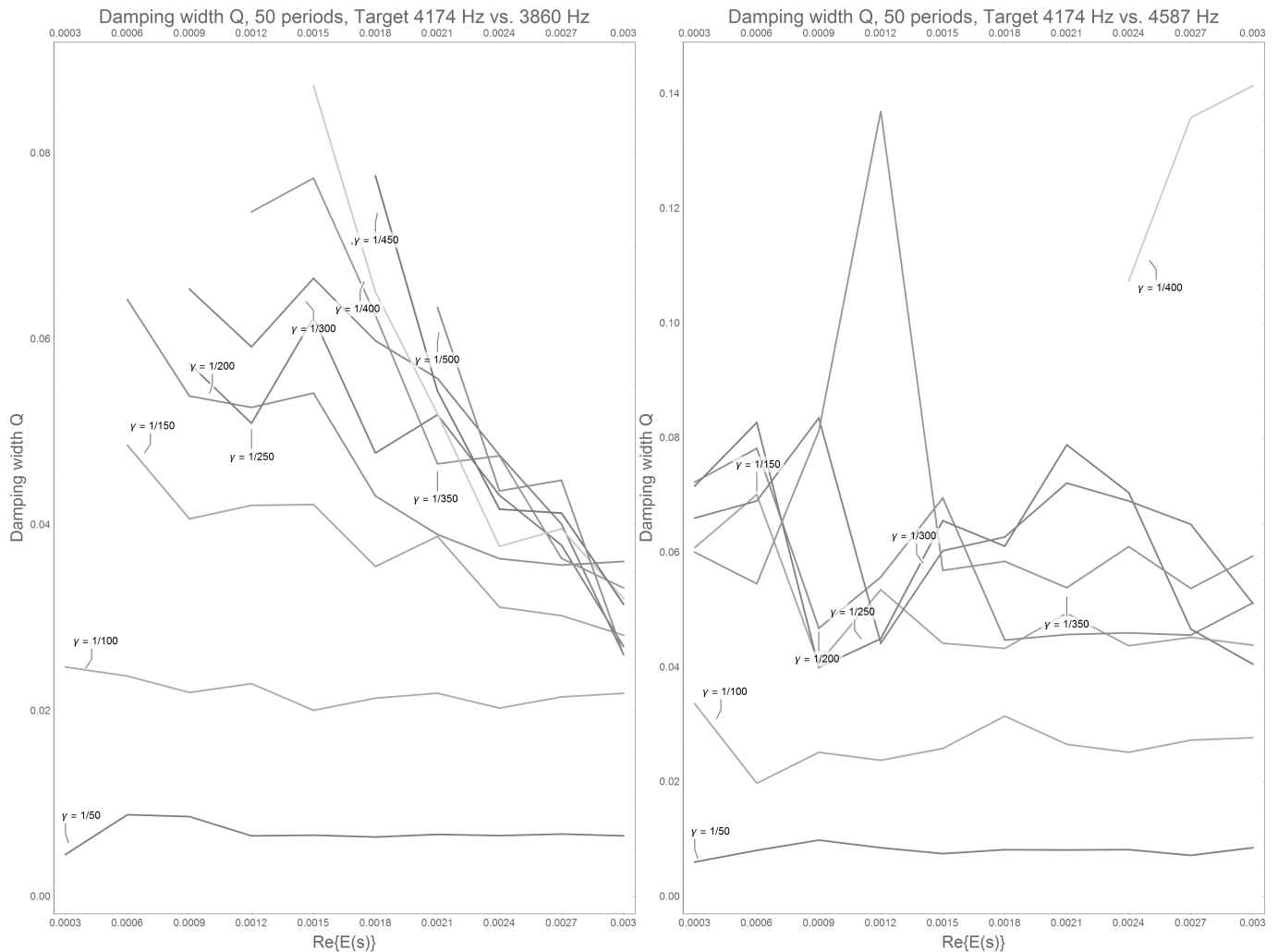


Figure 8: Same as Fig. 7, here for the 50 period case with lower  $\gamma$ . The basic pattern of larger  $Q$  with lower  $\gamma$  repeats, still in a more chaotic manner. This is due to very fast decay and the fact that the fitting of the damping curve to an exponential fit used to estimate  $\mu$ , from which  $Q$  is calculated becomes more problematic. The cases where the lines end (left plot high  $Q$ , low  $\gamma$  mean that there is no damping found anymore of the neighboring frequencies. Therefore here the damping  $Q$  is so sharp that it does no longer affect neighboring modes.

## REFERENCES

- [1] R. Bader, "Finite-Difference model of mode shape changes of the Myanmar *pat wain* drum circle using tuning paste", *Proc. Mtgt. Acoust.*, vol. 29, 035004, pp. 1-14 (2016).
- [2] R. Bader, "Nonlinearities and Synchronization in Musical Acoustics and Music Psychology," Springer-Verlag, Berlin, Heidelberg, *Current Research in Systematic Musicology*, vol. 2, pp. 157-284 (2013)
- [3] R. Bader, "Finite-element calculation of a bass drum," *J. Acoust. Soc. Am.*, vol. 119, pp. 3290 (2006).
- [4] I. Brémaud, J. Ruelle, A. Thibaut, and B. Thibaut, "Changes in viscoelastic vibrational properties between compression and normal wood : roles of microfibril angle and of lignin," *Holzforschung*, vol. 67(1), pp. 75-85 (2013).
- [5] I. Brémaud, "What do we know on " resonance wood " properties? Selective review and ongoing research," *Proceedings of the Acoustics 2012 Nantes Conference* (2012).
- [6] I. Brémaud, J. Gril, and B. Thibaut, "Anisotropy of wood vibrational properties: dependence on grain angle and review of literature data," *Wood Sci. Technol.*, vol. 45, pp. 735-754 (2011).
- [7] S. Bilbao, "Time-domain simulation and sound synthesis for the snare drum," *J. Acoust. Soc. Am.*, vol. 131 (1), pp. 914-925 (2012).
- [8] A. Chaigne, and Ch. Lambourg, "Time-domain simulation of damped impacted plates. I. Theory and experiments," *J. Acoust. Soc. Am.*, vol. 109 (4), pp. 1422-1432 (2001).
- [9] A.D. French, and G.P. Johnson, "Advanced conformational energy surfaces for cellobiose," *Cellulose* vol. 11 pp. 449-462 (2004).

- [10] Y.-F. Hwang, and H. Suzuki, "A finite-element analysis on the free vibration of Japanese drum wood barrels under material property uncertainty," *Acoust. Sci. & Tech.*, vol. 37 (3), pp. 115-122 (2016).
- [11] S. Jeyapalina, "Studies of the hydro-thermal and viscoelastic properties of leather," PhD, Univ. of Leichester (2004).
- [12] Maccaferri plastic guitar in the Museum of Arts and Applied Science, Sydney. Seen 13.5.2019: <https://maas.museum/inside-the-collection/2009/06/17/maccaferri-plastic-guitar/>
- [13] W. Müller, M. Käßner, J. Brummund, and J. Ulbricht, "On the numerical handling of fractional viscoelastic material models in a FE analysis," *Comput. Mech.*, vol. 51, pp. 999-1012 (2013).
- [14] L.M. Nickerson, and Th.D. Rossing, "Acoustics of the Karen bronze drums," *J. Acoust. Soc. Am.*, vol. 106, pp. 2254 (1999).
- [15] A.N. Norris, and D.M. Photiadis, "Thermoelastic Relaxation in Elastic Structures, with Applications to Thin Plates," *arXiv*, arXiv:cond-mat/0405323v2 [cond-mat.mtrl-sci] (2004).
- [16] E. Obataya, T. Umezawa, F. Nakatsubo, and M. Norimoto, "The effects of water soluble extractives on the acoustics properties of reed (*Arundo donax L.*)," *Holz-forschung*, vol. 53, pp. 63-67 (1999).
- [17] A. Pierce, "Intrinsic damping, relaxation processes, and internal friction in vibrating systems," *POMA*, vol. 9, pp. 1-16, (2010).
- [18] Th.D. Rossing, "Science of Percussion instruments." World Scientific, Singapore (2008).
- [19] G. Sathej and R. Adhikari, "The eigenspectra of Indian musical drums," *J. Acoust. Soc. Am.*, vol. 126 (2), pp. 831-838 (2009).
- [20] H. Suzuki and Y. Miamoto, "Resonance frequency changes of Japanese drum (nagado daiko) diaphragms due to temperature, humidity, and aging," *Acoust. Sci. & Tech.*, vol. 33 (4), pp. 277-278 (2012).
- [21] A. Tramer, Ch. Jungen, and F. Lahmani, "Energy Dissipation in Molecular Systems." Springer (2005).
- [22] R. Worland, "Demonstration of coupled membrane modes on a musical drum," *J. Acoust. Soc. Am.*, vol. 130, pp. 2397 (2011).
- [23] R. Worland, "Normal modes of a musical drum head under non-uniform tension," *J. Acoust. Soc. Am.*, vol. 127 (1), pp. 525-533 (2010).
- [24] P. Wriggers, "Nichtlineare Finite-Element Methoden. [Nonlinear Finite-Element Methods]," Springer (2001).
- [25] X.Q. Zhou, D.Y. Yu, X.Y. Shao, S.Q. Zhang, and S. Wang: "Research and applications of viscoelastic vibration damping materials: A review," *Composite Structures*, vol. 135, pp. 460-480 (2016).
- [26] X.Y. Zhou, D.Y. Yu, X.Y. Shao, S. Wang, and Y.H. Tian: "Asymptotic analysis on flexural dynamic characteristics for a sandwich plate with periodically perforated viscoelastic damping material core," *Composite Structures*, vol. 119, pp. 487-504 (2015).
- [27] X.Q. Zhou, D.Y. Yu, X. Shao, S. Wang, and Y.H. Tian:

"Band gap characteristics of periodically stiffened-thin-plate based on center-finite-difference-method," *Thin-Walled Structures*, vol. 82, pp. 115-123 (2014).

(Received May 1, 2020)



**Rolf Bader** Rolf Bader is professor for Systematic Musicology at the University of Hamburg. He also studied Physics, Ethnology, and Historical Musicology. After teaching at Stanford University as a Visiting Scholar is a lecturer for Systematic Musicology in Hamburg since 2007. His main research interests are Physical Modeling of Musical Instruments, Timbre and Rhythm Perception, Musical Signal Processing, Room Acoustics, or Music Ethnology. He also worked on Self-organization and Synergetics of Musical Instruments and Music Perception.

He is the editor of the Springer Handbook of Systematic Musicology, and wrote monographs like Computational Mechanics of the Classical Guitar (Springer 2005) or Nonlinearities and Synchronization in Musical Acoustics and Music Psychology. He is editor-in-chief of the Springer Series Current Research in Systematic Musicology where he also published a monograph, as well as the volume Sound-Perception-Performance and Computational Phonogram Archiving as an editor. He also works as an Ethnomusicologist mainly in Myanmar, Cambodia, China, India or Sri Lanka and is about to build up a Computational Ethnomusicological Sound Archive ESRA at his Institute. He is also a musician and composer in the fields of free improvised and electronic music, as well as Fusion and Rock, and published several CDs.